JLAB USER GROUP

Jefferson Lab PAC13
Proposal Cover Sheet

This document must be received by close of business Thursday, **December 18, 1997** at:

Jefferson Lab
User Liaison Office,
Mail Stop 12B
12000 Jefferson Avenue
Newport News, VA
23606

Experimental Hall: Hall C
Days Requested for Approval: 33

☒ **New Proposal Title:** Measurement of the (e,e'p) Cross section on Tensor Polarized Deuterium
☐ **Update Experiment Number:**
☐ **Letter-of-Intent Title:**
(Choose one)

Proposal Physics Goals
Indicate any experiments that have physics goals similar to those in your proposal.

A_{xx} for D(e,e'p)n

Approved, Conditionally Approved, and/or Deferred Experiment(s) or proposals:

Contact Person
Name: Heinz Anklin
Institution: Jefferson Lab A120
Address: Jefferson Ave 12000
Address:
City, State, ZIP/Country: Newport News VA 23602
Phone: 757-269 59 23 **Fax:** 757-269 58 00
E-Mail: Anklin@Cebaf.gov

JLab Use Only
Receipt Date: 12/18/97 PR-97-102
By: [illegible]

LAB RESOURCES LIST

JLab Proposal No.: ____________ Date ____________

(For JLab ULO use only.)

List below significant resources — both equipment and human — that you are requesting from Jefferson Lab in support of mounting and executing the proposed experiment. Do not include items that will be routinely supplied to all running experiments such as the base equipment for the hall and technical support for routine operation, installation, and maintenance.

Major Installations *(either your equip. or new equip. requested from JLab)*

polarized D, H target

New Support Structures:

chicane magnets

Data Acquisition/Reduction

Computing Resources:

New Software:

Major Equipment

Magnets: HMS, chicane, SOS out of plane

Power Supplies: standard

Targets: polarized target

Detectors: standard

Electronics: standard

Computer Hardware: standard

Other: standard

Other:

BEAM REQUIREMENTS LIST

JLab Proposal No.: ______________________ Date: ______________

Hall: ________ Anticipated Run Date: ______________ PAC Approved Days: __________

Spokesperson: ______________________ Hall Liaison: ______________________
Phone: ______________________
E-mail: ______________________

List all combinations of anticipated targets and beam conditions required to execute the experiment. (This list will form the primary basis for the Radiation Safety Assesment Document (RSAD) calculations that must be performed for each experiment.)

Condition No.	Beam Energy (MeV)	Mean Beam Current (μA)	Polarization and Other Special Requirements (e.g., time structure)	Target Material (use multiple rows for complex targets — e.g., w/windows)	Material Thickness (mg/cm²)	Est. Beam-On Time for Cond. No. (hours)
	2187	0.08	CW	pol. ND3, NH3	2640	42
	2076	"	"	"	"	69
	1917	"	"	"	"	88
	1688	"	"	"	"	137
	1495	"	"	"	"	170
	1330	"	"	"	"	200

The beam energies, E_{Beam}, available are: $E_{Beam} = N \times E_{Linac}$ where N = 1, 2, 3, 4, or 5. E_{Linac} = 800 MeV, i.e., available E_{Beam} are 800, 1600, 2400, 3200, and 4000 MeV. Other energies should be arranged with the Hall Leader before listing.

HAZARD IDENTIFICATION CHECKLIST

JLab Proposal No.: ______________________________ Date: ________________

(For CEBAF User Liaison Office use only.)

Standard Materials and Hazards for running in Hall C.

Check all items for which there is an anticipated need.

Cryogenics _____ beamline magnets _____ analysis magnets _____ target type: __________ flow rate: __________ capacity: __________	**Electrical Equipment** _____ cryo/electrical devices _____ capacitor banks _____ high voltage _____ exposed equipment	**Radioactive/Hazardous Materials** List any radioactive or hazadorous/ toxic materials planned for use: ____________________ ____________________ ____________________ ____________________
Pressure Vessels _____ inside diameter _____ operating pressure _____ window material _____ window thickness	**Flammable Gas or Liquids** type: __________ flow rate: __________ capacity: __________ **Drift Chambers** type: __________ flow rate: __________ capacity: __________	**Other Target Materials** ___ Beryllium (Be) ___ Lithium (Li) ___ Mercury (Hg) ___ Lead (Pb) ___ Tungsten (W) ___ Uranium (U) ___ Other (list below) ____________________ ____________________
Vacuum Vessels _____ inside diameter _____ operating pressure _____ window material _____ window thickness	**Radioactive Sources** _____ permanent installation _____ temporary use type: __________ strength: __________	**Large Mech. Structure/System** _____ lifting devices _____ motion controllers _____ scaffolding or _____ elevated platforms
Lasers type: __________ wattage: __________ class: __________ Installation: _____ permanent _____ temporary Use: _____ calibration _____ alignment	**Hazardous Materials** ___ cyanide plating materials ___ scintillation oil (from) ___ PCBs ___ methane ___ TMAE ___ TEA ___ photographic developers ___ other (list below) ____________________ ____________________	**General:** Experiment Class: _____ Base Equipment _____ Temp. Mod. to Base Equip. _____ Permanent Mod. to Base Equipment _____ Major New Apparatus Other: __________ __________

Jefferson Lab Proposal for the Measurement of the (e,e′p) Cross Section on Tensor Polarized Deuterium

H.C. Anklin(Co-Spokesperson), W.U. Boeglin(Spokesperson), L. Kramer, P.E. Markowitz, B.A. Raue
Physics Department
Florida International University
Miami FL 33199
Physics Division Jefferson Lab
Newport News, Virginia, 23606

J. Jourdan, M. Mühlbauer, I. Sick, G. Warren, J. Zhao
Department of Physics
University of Basel
CH-4056 Basel, Switzerland

R. Carlini, A. Lung, D. Mack, J. Mitchell
Physics Division Jefferson Lab
Newport News, Virginia, 23606

S. Bueltmann, J. McCarthy, D. Crabb, D. Day, O. Rondon, B. Zihlmann
Institute of Nuclear and Particle Physics
University of Virginia
McCormick Road
Charlottesville, VA 22901

December 17, 1997

1 Introduction

The structure of the ground state wave function in nuclei at small inter-particle distances is an experimentally as well as a theoretically unsolved problem. It is very important to obtain new experimental data in order to test realistic models which are able to predict the wave function at short distances. This will enable us to check as to how far the picture of the nucleus as composed of nucleons and mesons is valid since deviations from this description would indicate the need of including new degrees of freedom arising from the underlying quark structure.

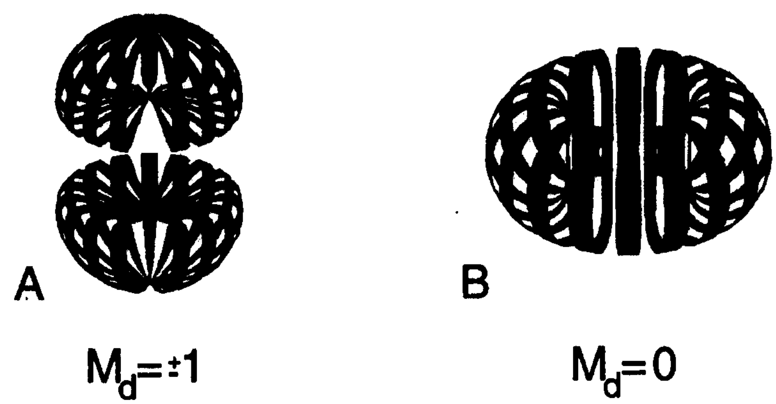

Figure 1: The equidensity surfaces of the $T = 0$ $S = 1$ two-nucleon distribution functions for $M_d = \pm 1$ (left) and $M_d = 0$ (right) from reference [1]

The short range structure of the ground state wave function is influenced by the repulsive core and the tensor part of the nucleon-nucleon interaction. A recent theoretical study [1] has shown that the two-nucleon distribution in the $T = 0$ isospin and $S = 1$ spin state have a strong dependence on the spin projection M_d. If the two nucleons are in a relative $M_d = 0$ state, the surface of constant density has the shape of a toroid while if the two nucleons are found in the $M_d = \pm 1$ state the surface of constant density has a dumbbell shape. The two nucleon density is at a maximum in the $M_d = 0$ state for a torus with a diameter of approximately 1 fm. The shape of the torus is produced by the combined action of the tensor force and the repulsive core which is responsible for the hole.

The deuteron is the prime target to start this investigation because its structure can be calculated with high precision using realistic nucleon nucleon potentials and its ground state is in the $S = 1$ and $T = 0$ state. The equidensity surfaces of the deuteron from reference [1] are shown in figure 1. Experimental information about the thickness and the diameter of the torus can be extracted from the t_{20} and from the magnetic form factor of the deuteron. However these measurements alone cannot give all the necessary information about the origin of the observed structure. Indeed equidensity surfaces for the deuteron, toroidal in shape, have also been predicted by the Skyrme model of QCD [2].

It is important to realize that elastic form factor measurements alone can not discriminate between this picture of the nucleus and the more conventional one based on nucleonic degrees of freedom. It is especially interesting to obtain information about whether two nucleons

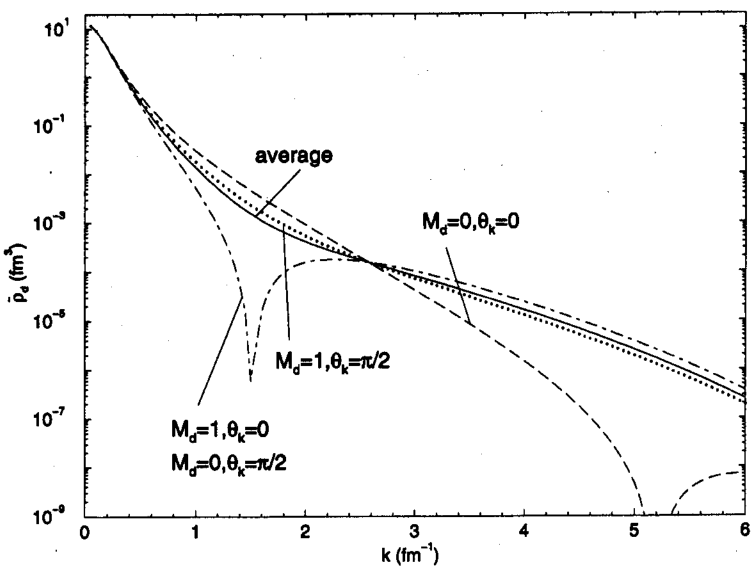

Figure 2: The calculated deuteron momentum distribution for different values of M_d and θ_k from reference [1]

which are only 1 fm apart remain in pure nucleon states. In this (toroidal) configuration they have considerable overlap, given the rms proton charge radius of 0.8 fm.

The necessary additional information can be obtained from measurements of M_d dependent (e,e′p) coincidence cross section. If final state interactions are neglected (PWIA) the cross section can be written as follows:

$$\frac{\mathrm{d}^6\sigma}{\mathrm{d}\omega \mathrm{d}\Omega_e \mathrm{d}\Omega_p \mathrm{d}T_p} = K \cdot \sigma_{ep} \cdot S(E, p_i)$$

where σ_{ep} is the (off-shell) electron nucleon cross section which describes the scattering off a moving (bound) nucleon and $S(E, p_i)$ is the spectral function which corresponds in the deuteron case to the momentum distribution $\rho(p_i)$ with p_i the initial momentum of the nucleon. Scattering off polarized Deuterium can be described by replacing $\rho(p_i)$ by angular momentum projection (M_d) dependent momentum distribution $\rho(p_i)^{0,\pm1}$.

The calculated $\rho(p_i)^{M_d}$ for the different M_d states is shown in figure 2. The angle θ_k is the angle between the momentum $\vec{p_i}$ and the quantization axis. Within the limits of PWIA using a polarized target permits in principle the determination of the polarization dependent momentum distribution. If the nucleons really remain nucleons as described above, then the momentum distribution must have this dependence on the deuteron orientation.

In a full calculation where final state interactions and meson exchange currents are taken into account the minimum at $p_i = 1.4 fm^{-1}$ is filled and one obtains the cross sections shown in figure 3. We intend to measure the M_d dependent coincidence cross section for p_{miss} -values between 200 MeV/c and 400 MeV/c. In this region the momentum distribution is dominated by the D-state wave function which due to the tensor force is part of the deuteron ground state wave function. The calculation used in this proposal includes final state interaction and meson exchange currents. As figure 4 shows it can reproduce very well un-separated

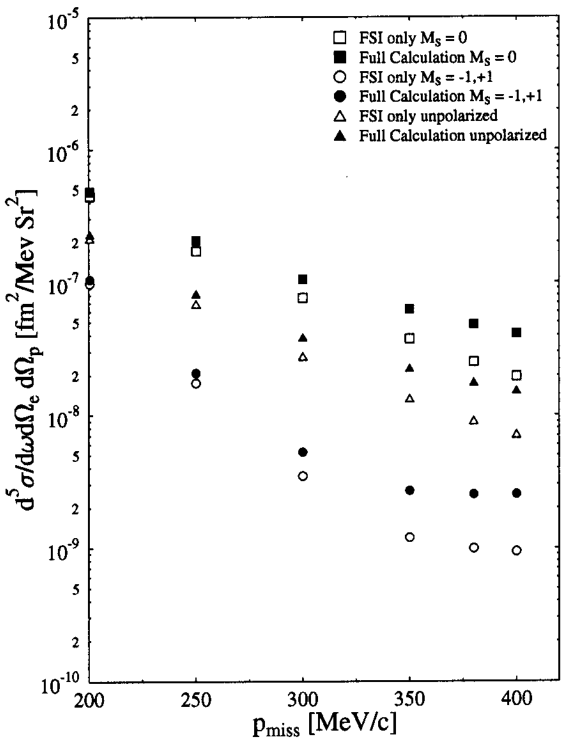

Figure 3: The calculated coincidence cross section [4] for the D(e,e′p)n reaction for $M_d = 0$ and $M_d = \pm 1$ states and the unpolarized cross section.

(e,e'p) cross sections measured in Mainz on the deuteron which cover the same region of missing momenta. In this example the momentum transfer was 600 MeV/c [3] It is the goal of this experiment to separate the D(e,e'p)n cross sections for the $M_d = 0$ and $M_d = \pm 1$ states for missing momenta ranging from 200 MeV/c to 400 MeV/c.

2 Outline of Experiment

Using a tensor polarized deuterium target, we propose to measure the tensor analyzing power A_{xx} (fig. 5 [4]) and the unpolarized cross section of the $D(e, e'p)n$ reaction at a momentum transfer of 500 MeV/c in parallel kinematics. The hall C spectrometers will be used to measure the scattered particles in coincidence. Electrons will be detected in the short orbit spectrometer (SOS) and protons will be measured in the high momentum spectrometer (HMS). Six measurements are planned to cover a range in missing momentum from 200 MeV/c to 400 MeV/c.

With the knowledge of both, A_{xx} and the unpolarized cross section, the individual cross sections for scattering off the deuteron in the M_s=0 and in the M_s=±1 spin sub-states can be determined.

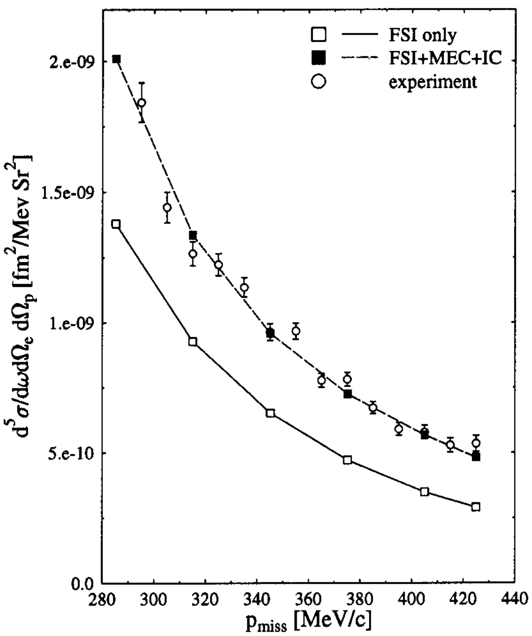

Figure 4: The calculated coincidence cross for the D(e,e'p)n reaction for $\vec{q}\ = 600 MeV/c$ compared to data measured in Mainz [3].

2.1 Kinematics

Table 1 shows the selected kinematical settings. They have been chosen in order to minimize the requested beam time by minimizing the electron scattering angle. The minimal angle of the SOS has been taken from the SOS handbook. The orientation of the Helmholtz field has been chosen along $\vec{q}$ where possible. However the opening angle of the target bore does not allow this for the missing momenta of 300 MeV/c and less. Therefore the closest possible orientation has been chosen with the quantization axis still in the scattering plane (table 2). The effect on A_{xx} is in a first approximation a reduction of the effective polarization according to the expression $\frac{1}{2}(3cos\theta_{Bq} - 1)$, where the angle θ_{Bq} is the angle between the $\vec{B}$-field and the momentum transfer. For the smallest missing momentum measured (200 MeV/c) we obtain an angle $\theta_{Bq} = 20°$ and a corresponding reduction factor of 0.8 and for a missing momentum 300 MeV/c the reduction factor is only 0.93.

2.2 Determination of A_{xx}

A_{xx} is determined from relative cross section measurements with the target tensor-polarized and unpolarized in the same setup. For the unpolarized measurement the target polarization will be destroyed by warming the target up. After this procedure the target material will be cooled down again to the previous temperature in order to have the same density as for the polarized measurement, but without the transition inducing microwave radiation.

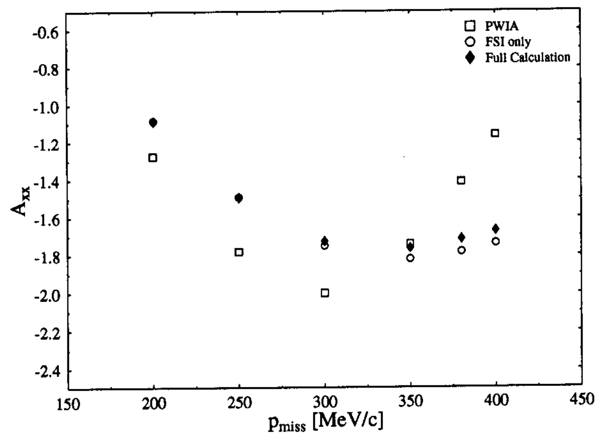

Figure 5: Tensor analyzing power A_{xx} as a function of the missing momentum (p_m in parallel kinematics. The difference between the PWIA result and the full calculation is manly due to final state interactions.

Setting Nr.	p_m $\frac{MeV}{c}$	E_{beam} MeV	Θ_e deg	ω MeV	q $\frac{MeV}{c}$	Θ_q deg	p_f $\frac{MeV}{c}$
1	200	2187	12	256	500	53.44	700
2	250	2076	12	298	500	47.67	750
3	300	1917	12	344	500	40.87	800
4	350	1688	12	393	500	32.57	850
5	380	1495	12	424	500	26.45	880
6	400	1330	12	445	500	21.56	900

Table 1: Central kinematic settings

For the configuration used in this experiment, where the quantization axis is in the scattering plane A_{xx} is determined by

$$A_{xx} = \frac{2}{p_{zz}}\left(\frac{N_{pol}}{N_{unpol}} - 1\right), \tag{1}$$

where N_{pol} and N_{unpol} are the number of counts with beam on the polarized and the unpolarized target after they have been normalized to the same accumulated charge. P_{zz} is the tensor polarization of the target. The M_s dependent cross sections are obtained as follows:

$$\sigma_{M=-1} = \sigma_{M=+1} = \sigma_{unpol}(1 + \frac{1}{2}A_{xx}) \tag{2}$$

$$\sigma_{M=0} = \sigma_{unpol}(1 - A_{xx}) \tag{3}$$

The measurement of A_{xx} allows a separation of the unpolarized cross section in $\sigma_{M=0}$ and $\sigma_{M=\pm1}$ The unpolarized cross section will be determined from the measurements on the unpolarized target.

3 Polarized Target

We will use the polarized ND_3 target of UVA and the University of Basel with tensor polarized deuterons. The target is completely operational since August 1992. It has already been successfully used in SLAC experiments [8] at beam currents up to 100nA and is in the process of being installed at Jefferson Lab in hall C for the measurement of the electric form factor of the neutron [9].

With ND_3 targets, tensor polarizations of 22% have already been achieved in previous experiments [6]. With a similar technique as has already been employed in the existing target to maximize the deuteron vector polarization [5] we expect to be able to obtain a tensor polarization of at least 20% by inducing the specific transitions leading to the M_s=0 state. The tensor polarization of the target will be measured using NMR techniques as described in ref [7] by analyzing the NMR line shape. We expect to be able to measure the tensor polarization with a relative precision of 7%.

As can be seen in figure 8, a tensor polarization of only 12%, already allows a meaningful experiment. This can be understood, when one takes into account that the observed tensor analyzing power A_{xx} has a maximum near p_m = 350 MeV/c and is there approximately -1.8 (figure 5).

The schematic of the polarized target assembly is shown in figure 6. The target is surrounded by a split Helmholtz coil which produces a longitudinal field of 5.1 T. The target is operated at a temperature of 1K. The mechanical design of the magnet allows an opening angle of ± 50 degrees with respect to the field direction. A detailed description can be found in reference [9] and [5].

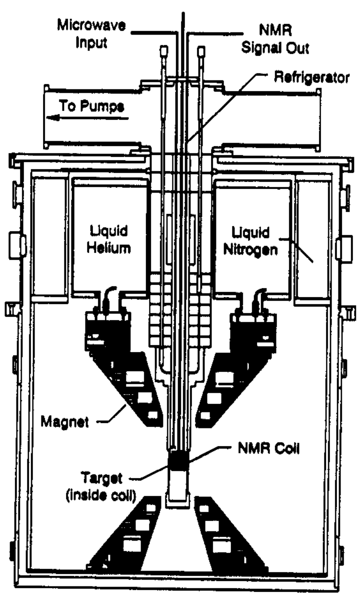

Figure 6: Schematic view of the polarized target.

When using a polarized target, the holding field deflects all charged particles entering and exiting the target. For a complete optimization of the experimental setup it is crucial to study the effect of the holding field of the target on the electron beam, the scattered electrons and the break-up protons.

We therefore have set up a simulation using the GEANT Detector Description and Simulation Tool and a measured field map of the super-conducting magnet. This simulation allows us to precisely optimize and study the acceptance of the experimental setup. Since

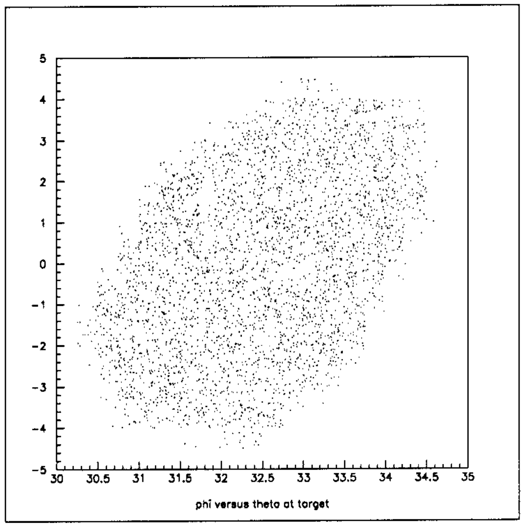

Figure 7: Theta versus phi of the scattered protons that enter HMS.

the magnetic field is in the scattering plane along the direction of the outgoing protons, only a small deflection of the protons will be observed. Figure 7 shows the proton scattering angles that enter the HMS Spectrometer. It can be seen that the scattered protons follow a helix around the quantization axis (the solid angle appears to be rotated).

With $\vec{B}$ along $\vec{q}$, the scattering plane is restricted to the horizontal plane. The orientation of the magnetic field versus the beam has been chosen in order for the scattered electrons to be deflected upwards. This makes it necessary to detect the scattered electrons in the SOS spectrometer with out-of-plane angles ranging from 4.9 to 7.8 degrees. The detection of the scattered electrons out of the electron scattering plane allows us to detect protons with HMS in parallel kinematics since the electron scattering plane is still parallel to the hall floor. The necessary out of plane angles are still well within the range of angles the SOS has originally been designed to be able to measure (up to 20 degrees).

To compensate for the deflection of the beam(table 2) the hall C chicane magnets will be used. The chicane will produce a horizontally incident beam at the center of the polarized target similarly to the G_n^E-measurement [9] except that G_n^E requires an upward and for this experiment we need a downward incoming beam. Modifications to the support of the chicane magnets are necessary in order to provide a downward incoming beam.

E_{beam} MeV	$\theta_{\vec{B}}$ deg.	beam deflection deg.
2187	32.6	3.2
2076	32.6	3.3
1917	32.6	3.6
1688	32.6	4.1
1495	26.5	3.7
1330	21.6	3.4

Table 2: Deflection angles of the incoming beam in degrees.

3.1 Cross Sections Measurements and Calibrations

In order to determine the target asymmetry A_{xx} an absolute knowledge of the target thickness is not necessary. Instead one needs a precise relative measurement of the polarized and the unpolarized cross sections. Therefore relative variations of the target thickness have to be monitored. The relative Deuterium contents can be measured during the experiment since we also measure the (e,e'p) cross section off nitrogen simultaneously with the deuteron cross section. The absolute deuteron contents can be measured by means of elastic electron scattering off the Deuterium in ND_3.

The $\vec{D}(e,e'p)n$ reaction can be separated from the ^{15}N(e,e'p) reaction by calculating the missing energy using a neutron as recoiling particle. In this case we will obtain a sharp peak for the $\vec{D}(e,e'p)n$ reaction and a continuum for the ^{15}N(ee'p) process.

The missing energies for the ^{15}N(ee'p) reaction associated with the $\vec{D}(e,e'p)n$ kinematics range from 20MeV (for $p_{miss} = 200$ MeV/c) to 80 MeV (for $p_{miss} = 400$ MeV/c). For the low missing momentum region, this corresponds to nucleon knock out from the S-shell of ^{15}N. An estimate of the background coincidence rate from the ^{15}N(ee'p) reaction gives a rate in a missing energy bin of 5 MeV of about 15% of the deuteron rate. For this estimate we have used the spectral function of the $^{12}C(e,e'p)$ reaction measured at NIKHEF [11]. To estimate the Nitrogen contribution to the coincidence cross section at large missing momenta we used the experimental spectral function measured at Mainz for ^{16}O[10] at missing momenta centered around 350 MeV/c. We expect for a missing momentum of 380 MeV/c in a missing energy bin of 5 MeV a rate which is about 20% of the deuteron rate. As mentioned above the nitrogen coincidence cross section can also be used to monitor variations in the target thickness.

In addition the nitrogen background can also be measured using a NH_3 target and subsequently be subtracted from the corresponding missing energy spectrum for ND_3.

4 Error Estimation

The statistical precision has been set to 1% for the measurement on the polarized and on the unpolarized target. This leads to a statistical error in A_{xx} of ± 0.123 (7.2%) at a missing momentum of 300 MeV/c. With the tensor polarization of 0.2 known to 7% the total error in A_{xx} amounts to ± 0.172 (10%). Assuming a one percent determination of the unpolarized cross section the resulting error in the determination of $\sigma_{M=0}$ is 6.7×10^{-9} (6.4%). The error in $\sigma_{M=\pm1}$ amounts to 3.3×10^{-9}. The following formula has been used to calculate the error of $\sigma_{M=0(\pm1)}$:

$$\Delta\sigma_{M=0(\pm1)} = \sqrt{(\frac{\delta\sigma_{M=0(\pm1)}}{\delta A_{xx}} * \Delta A_{xx})^2 + (\frac{\delta\sigma_{M=0(\pm1)}}{\delta\sigma_{unpol}} * \Delta\sigma_{unpol})^2}$$

Figure 8 shows the relative error of $\sigma_{M=0}$ as a function of the tensor polarization p_{zz} with p_{zz} known to 7%. Figure 9 shows the relative error of $\sigma_{M=0}$ as a function of the relative error

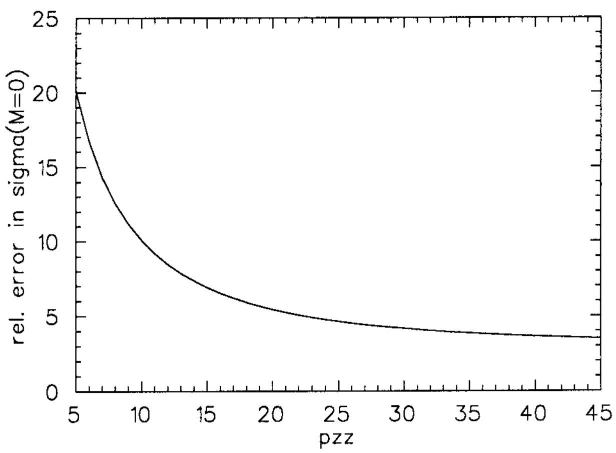

Figure 8: Relative error of $\sigma_{M=0}$ as a function of the tensor polarization p_{zz}.

in p_{zz} with $p_{zz} = 0.2$. Taking into account the expected precision of the tensor polarization

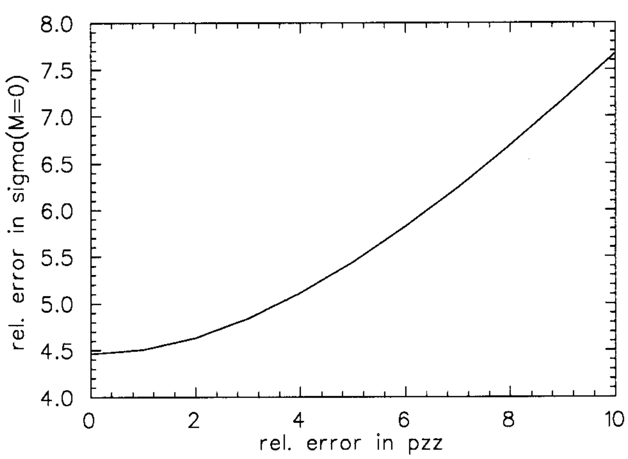

Figure 9: Relative error of $\sigma_{M=0}$ as a function of the relative error in p_{zz} at $p_{zz} = 20\%$.

measurement of 7% and a statistical error of 1% in each cross section measurement we expect the errors in the target asymmetry A_{xx} as shown in figure 10. Using the absolute cross sections measured one can then expect the following values for the M_S-dependent cross sections(figure 11). The error bars for the $M_S = 0$ state are smaller than the data point shown.

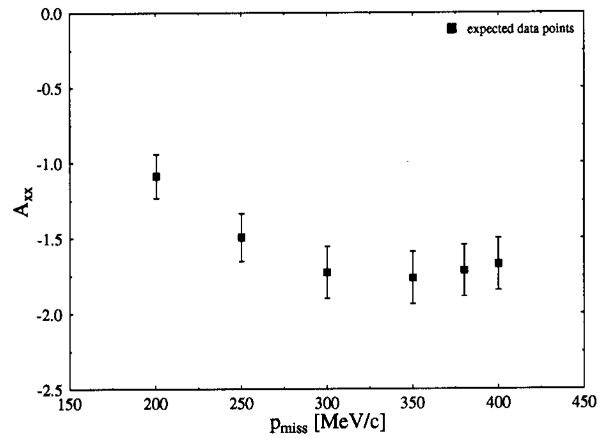

Figure 10: Expected data points for the asymmetry A_{xx}.

5 Count Rate and Beam Time Estimates

An event generator for $\vec{D}(e, e'p)n$ has been included in the GEANT simulation. This allows us to determine the coincident rates using a coincidence cross section which has been averaged over the detector acceptance. It also allows us to determine the detector acceptance volumes for each setting including the effect of the strong magnetic field at the target. The result of these Monte Carlo calculations are then used to calculate the expected rates and the necessary beam time. The electron single arm cross sections (table 3 have been calculated using the program QFS [12] and the hadron single arm cross sections have been determined with EPC [12]). For the measurements with the polarized target we have assumed a beam current of 80 nA and a coincidence time bin width of 5 ns. It is expected, that the measurements with the unpolarized target can be done with a beam current of 160nA.

The rates are calculated for a missing momentum bin width of 40MeV/c. The momentum acceptance of the spectrometers used was ±8% in order to minimize the effects due to solid angle variations as a function of particle momentum. To estimate the signal to noise ratio, we used the full range in missing momentum as measured by the two spectrometers with the selected momentum acceptances. Table 3 shows the deuteron coincidence cross sections and the single arm cross sections calculated for the corresponding kinematics.

Setting Nr.	p_m $[\frac{MeV}{c}]$	$\sigma_{D(ee'p)}$	$\sigma_{D(ee')}$	$\sigma_{N(ee')}$	$\sigma_{D(ep)}$	$\sigma_{N(ep)}$
1	200	2.04	20	109	1.1	13.0
2	250	0.72	11	97	1.0	11.2
3	300	0.29	15	93	1.1	10.4
4	350	0.13	19	114	1.1	10.3
5	380	0.086	18	126	1.2	10.2
6	400	0.06	16	131	1.1	9.8

Table 3: Cross sections are in nb. Single cross sections have been calculated using QFS and EPC. All cross sections have been averaged over the acceptances.

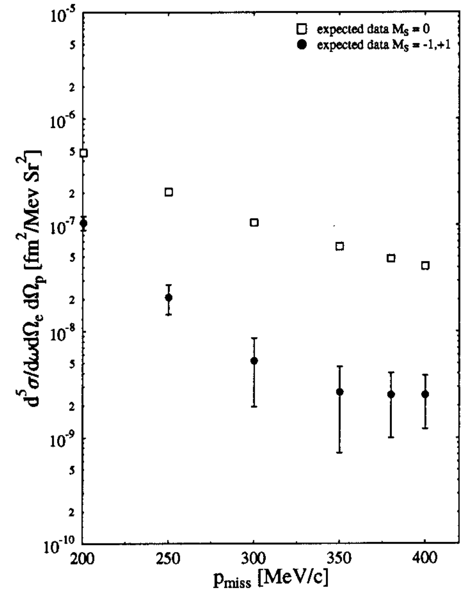

Figure 11: Expected data points for the M_S-dependent cross sections.

We obtain signal to noise ratios for the D(e,e′p)n reaction ranging from 3 to 100 depending on the selected kinematics (table 4). The calculated beam time in table 4 do not include radiation losses and time for unpolarized measurements. For the calculation of the total beam time a correction factor for radiative losses of 1.3 has been applied. For the measurement of the averaged (unpolarized) cross section an additional factor 1.5 has been applied.

Setting Nr.	p_m $\frac{MeV}{c}$	coincidence rate Hz	e single rate Hz	p single rate Hz	signal to noise ratio	beam time h
1	200	0.26	16000	67	100	11
2	250	0.12	8820	114	61	25
3	300	0.09	10050	185	18	35
4	350	0.06	10060	261	6	60
5	380	0.05	8860	345	4	77
6	400	0.04	7360	415	3	90

Table 4: Count rates have been estimated using HMS and SOS with a used momentum acceptance of ±8% each, a p_{miss} bin width of 40 MeV/c and a beam current of 80 nA.

We plan to measure the unpolarized cross section every 12 hours in order to minimize possible systematic errors due to slow variations in the target thickness and the deuterium content of the target material. We estimate a total 120 hours are necessary for target manipulations (polarizing, depolarizing, heating, cooling, annealing) during the experiment.

6 Summary

In this experiment we can measure new observables of the deuteron electro-disintegration which have been inaccessible up to now and are expected to provide new insights into the structure of the deuteron and the short-range behavior of nucleons in nuclei.

This experiment requires significant modifications and additions to the currently available equipment in Hall C. The most important one is the ability to detect electrons out of the conventional electron scattering plane (parallel to the hall floor). The other important modification concerns the ability to position the SOS at the smallest forward angle possible. While the out-of-plane capability is absolutely necessary for this experiment, there exists some flexibility in the minimal electron scattering angle at the cost of beam time and/or statistical precision. Below (table 5) we provide a summary of the beam time requested including calibrations, angle changes, beam energy changes and target manipulations

data taking (polarized and unpolarized) including corrections for radiative losses	579
target manipulations and calibrations	120
beam energy changes	40
elastic runs and angle changes	48
TOTAL	787

Table 5: Summary of requested time (hours)

References

[1] J.L. Forest, V.R. Pandharipande, S.C. Pieper, R.B. Wiringa, R. Schiavilla and A. Arriaga, Phys. Rev. C 54 646 (1996)

[2] R.A. Leese, N.S. Manton and B.J. Schroers, Nucl. Phys. B442, 228 (1995)

[3] K.I. Blomqvist et.al. to be published in Phys. Lett. B, W.U. Boeglin private communications.

[4] R. Schiavilla private communications.

[5] T.D. Averett, et.al. to be published in NIM

[6] W. Meyer et.al. NIM A244 (1986), 574

[7] C. Dulya et.al., NIM A398 (1997), 109

[8] K. Abe et al. Phys. Rev. Lett. 75 (1995) 25, K. Abe et al. Phys. Rev. Lett. 76 (1996) 587

[9] D. Day et.al. The Charge Form Factor of the Neutron, CEBAF proposal PR93-026 (1993)

[10] K.I. Blomqvist et.al. Phys. Lett. B344 (1995)85

[11] G. van der Steenhoven et al. Nucl.Phys A484 (1988)445

[12] J.W. Lightbody and J.S. O'Connell, Modeling single arm electron scattering and nucleon production from nuclei by GeV electrons, Computers in Physics, May/June (1988) 57